Hindawi
Adsorption Science & Technology
Volume 2022, Article ID 8110436, 15 pages
https://doi.org/10.1155/2022/8110436

Research Article

Artificial Intelligence-Based Tools for Process Optimization: Case Study—Bromocresol Green Decolorization with Active Carbon

Gabriel Dan Suditu,[1] **Elena Niculina Drăgoi**,[1,2] **Alexandra Georgiana Apostică**,[1] **Andra Maria Mănăilă**,[1] **Veronica Mădălina Radu**,[1] **Adrian Cătălin Puițel**,[1] **and Mircea Teodor Nechita**[1]

[1]*Faculty of Chemical Engineering and Environmental Protection "Cristofor Simionescu", "Gheorghe Asachi" Technical University of Iași, Bd. Prof. Dimitrie Mangeron, No. 73, 700050 Iași, Romania*
[2]*Faculty of Automatic Control and Computer Engineering, "Gheorghe Asachi" Technical University of Iași, Bd. Prof. Dimitrie Mangeron, No. 73, 700050 Iași, Romania*

Correspondence should be addressed to Mircea Teodor Nechita; mircea-teodor.nechita@academic.tuiasi.ro

Received 10 March 2022; Accepted 14 July 2022; Published 30 July 2022

Academic Editor: Mahmoud Nasr

This study highlights the benefits of optimizing the decolorization of bromocresol green (a colorant/pH indicator widely used in the industry, whose degradation produces toxic byproducts) by adsorption on active carbon. A set of experiments were planned and performed based on the design of experiments methodology for the following parameters: the colorant concentration (0.009-0.045 g/L), the amount of adsorbent (0.5-3 g/L), and the contact time (60-240 min). Modeling and optimization strategies were employed to determine the working conditions leading to efficiency maximization. Using the response surface methodology, the optimum values of the primary process parameters were established. In addition, a modified bacterial foraging optimization algorithm was applied as an alternative optimizer in combination with artificial neural networks in order to determine multiple combinations of parameters that can lead to maximum process efficiency. Different solutions were obtained with the considered strategies, and the maximum efficiency obtained was >99%. The study emphasizes that adsorption on active carbon is an effective method for bromocresol green decolorization in wastewater that can be further improved using advanced optimization methods.

1. Introduction

For thousands of years, the dyes and the pigments used were derived from natural sources. Only in the middle of the 19th century, when the natural resources were insufficient to fulfill the increasing demand, did the genuine industry of synthetic dyes and pigments start to grow [1–6]. Nowadays, the production of dyes and pigments has reached millions of tons per year [7], and almost every industry is a consumer. On a global scale and in a relatively short time, such tremendous growth generated massive amounts of air, water, and soil pollutants [8–11].

Many manufacturing branches generate colored industrial wastewaters such as dye industries, Kraft bleaching, tannery, textiles, pulp and paper, food processing, cosmetics, and pharmaceuticals [12, 13]. Consequently, over the years, numerous physicochemical treatments and decolorization methods have been proposed [14, 15]: coagulation and flocculation [16], electrocoagulation [17], adsorption [18–21], wet oxidation [22], ozonation [23], photochemical degradation [24], biodegradation [25], and other advanced oxidation processes [22], with each method having its own advantages and drawbacks [26]. To be competitive, all these methods must evolve with the technical progress and the continuous tightening of the environmental standards and regulations [27]. In this view, there are a series of directions that focus on (i) finding new, more effective technologies [28, 29], (ii) combining existing methods to increase their effectiveness

[30–33], and (iii) optimizing existing technologies to increase the efficiency and decrease the operation costs [34, 35].

One of the classical approaches with multiple applications in the optimization of industrial wastewater treatments [23, 24, 36–38] is the response surface method (RSM) based on central composite design (CCD), proposed in the '60s by Box and Hunter [39]. RSM is based on a collection of statistical and mathematical techniques (helpful in developing, improving, and optimizing processes) that is widely used to design an experiment, explain the main interaction effects of the independent variables, and determine the optimal conditions using a limited number of experiments [40–42]. On the other hand, artificial neural networks (ANNs), although proposed roughly during the same period as RSM, has recorded in the latest years a series of breakthroughs that demonstrated their extraordinary potential to model complex systems with highly nonlinear interactions. Therefore, ANNs have a large area of applicability, being applied to many fields. Examples in the adsorption area include (i) ultrasonic-assisted adsorption [43], (ii) dye adsorption [44], and (iii) heavy metal biosorption [45]. However, despite their advantages and capabilities, ANNs suffer from several drawbacks related to the model type and hyperparameter tuning [46, 47], which depend on the problem's characteristics. In this context, neuroevolution (combining ANNs with evolutionary-based algorithms) is a strategy that can be used to overcome these problems, with the hyperparameter optimization being performed by the optimization strategy.

For the optimization step of this study, a population-based algorithm represented by bacterial foraging optimization (BFO) was used. BFO [48] is a bioinspired metaheuristic that mimics the foraging behavior of *E. coli*. Among the multitude of nature-inspired algorithms [49], BFO distinguished itself as an efficient approach. Its simplicity, ease of use, and efficiency in solving a wide range of problems represent the main reasons for selecting BFO from the multitude of algorithms from its class [34] and applying it as an alternative approach to RSM for optimizing the considered process. Furthermore, it was successfully applied to various synthetic [50, 51] and real-world problems [52].

Various types of adsorbents: conventional [53, 54], non-conventional [55], ion-exchange [56], and biosorbents [57], were employed in decolorization of dye-polluted wastewaters [58]. Although rather costly, activated carbon is generally recognized as one of the most efficient adsorbents that can be successfully used for various colored or noncolored pollutants [26].

Typically, the chemicals that generate the effluent's color absorb light, directly impacting photosynthesis. They also reduce visibility, making it more difficult for microorganisms to eat or reproduce [59]. Bromocresol green (BCG) is a member of the triphenylmethane (anionic) family and has a variety of applications as a pH indicator, DNA tracer, and tracking dye in the weaving industry (cotton, flax) [60, 61]. However, the three benzene rings' molecular structure makes it difficult to degrade once released into wastewater naturally. As a result, there are numerous studies related to its complete removal and/or decolorization using various methods [62–66]. Among these, two strategies attract much attention: advanced oxidation processes (AOPs) and adsorption on activated carbons (AC) or other materials such as chitin [61] or polymers [67]. The AOPs usually involve chemically assisted UV irradiation [68, 69] and/or heterogeneous photocatalysis [70, 71]. As for the active carbon-based materials, the focus is on preparing activated carbon from various low-value natural materials [72, 73] using pyrolysis and, in some cases, additional chemical activation [34]. Although this method is one of the most cost-effective, the properties of the resulting AC are highly dependent upon the conditions under which the raw material is produced (soil quality, precipitation, temperature, etc.).

As a result, this research focuses on commercial AC with controlled and repeatable properties. This research is aimed at evaluating the AC's capacity for BCG decolorization and underlining that process optimization using artificial intelligence-based strategies can improve process efficacy. In this context, the interaction among three parameters (the BCG concentration, the amount of adsorbent, and the contact time) and their influence on the process yield was analyzed, modeled, and optimized using RSM, ANNs, and a BFO-based approach. The variant of BFO used in this work is a modified, improved version. In order to distinguish between the two versions, the standard algorithm will be referred to as BFO, while the modified version will be denoted as iBFO. Graphical response surface and contour plots were used to identify the best operating conditions. This work's novelty consists of applying classic (RSM) and newer modeling and optimization methods (ANNs, iBFO) for improving the bromocresol green decolorization using active carbon. Moreover, to the author's knowledge, iBFO has never been applied to such a process.

2. Materials and Methods

2.1. Work Plan. This study is aimed at showing that even classical and well-known processes (e.g., colorant adsorption on active carbon) can be improved by using a combination of (i) standard approaches for planning, modeling, and optimization and (ii) artificial intelligence techniques that combine ANNs with bioinspired metaheuristic optimizers. Consequently, the knowledge about the considered process was gathered through experimental analysis and planned using a design of experiment (DOE) approach. Then, the process was modeled using two approaches (RSM and ANNs). Finally, the process optimization was performed by two distinct strategies (RSM and iBFO). Figure 1 presents the main workflow of data and the interconnection between all the applied strategies.

2.2. Materials. BCG powder (analytical purity, supplied by S. C. ChimReactiv Ltd.) and bidistilled water were used to prepare the dye solutions. Irregular-shape particles of active carbon, supplied by Romcarbon S.A., were used to perform the experiments. Before performing the experiments, the particles were washed several times with bidistilled water to remove surface impurities, dried at 120°C for 24 h, and

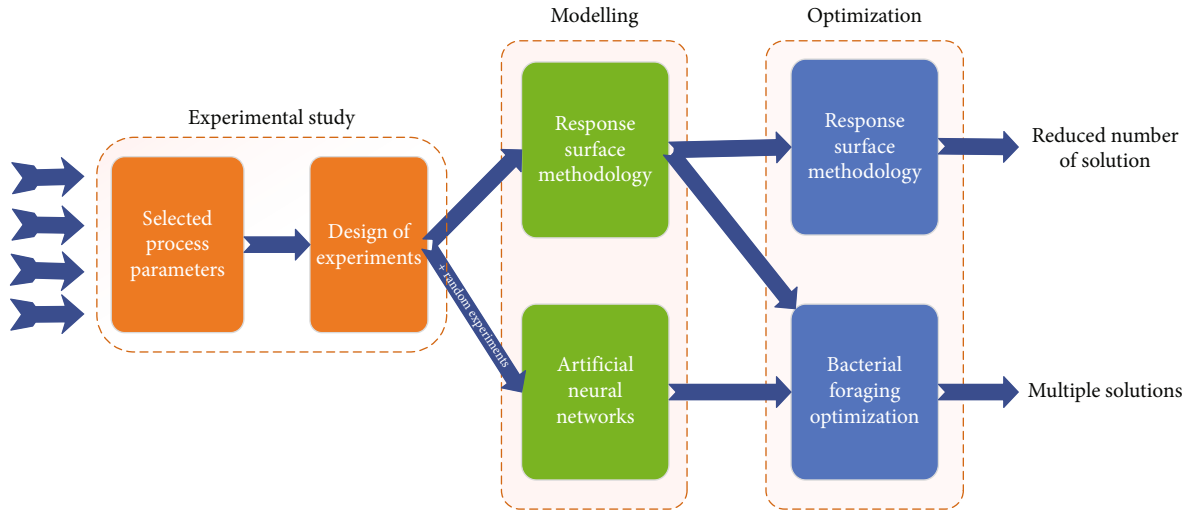

Figure 1: Workflow for the application of the different strategies used in this work.

Table 1: The specific surface areas and porous characteristics of commercial activated carbon.

Physical properties	Characteristics	Value
Surface	BET surface	1403 m^2/g
	External surface	38 m^2/g
	Total surface	631 m^2/g
	Mean pore size	1.62 nm
Volume	Specific microporous volume	0.48 cm^3/g
	Total microporous volume	0.66 cm^3/g

classified by sieving; the average diameter ranges between 2.5 and 3.15 mm.

The main characteristics of the commercial active carbon (Table 1) were investigated by Secula et al. [74]. In addition, for this study, SEM images were registered (Figure 2). The captured images emphasized the parallel arrangement of the pores and their size similarity (Figure 2(b)). In addition, the micropores are perpendicularly placed on the macropores (Figure 2(a)).

2.3. Experimental Design. In order to determine the optimal parameters for BCG decolorization, three independent variables were considered based on the experience of our previous studies [34, 75]. Table 2 presents the considered variables, their unit of measure, and the considered range used in the experimental phase based on DOE.

The UV-Vis spectra and the absorbance values were recorded using a JASCO V-550 UV-Vis spectrophotometer. Disposable disc filters of 0.45 μm were used for particle separation during solution sampling. The morphologies of the AC particles were observed using a Vega-Tescan scanning electron microscope.

Following the DOE procedure proposed by Box and Hunter [39], a minimum number of relevant experiments were statistically identified (Table 3) and further used in the experimental analysis.

2.4. Experimental Procedure. Batch adsorption experiments were performed using 100 mL solution samples with the required BCG concentration without additional pH adjustments. The solutions were mixed with an adequate amount of active carbon for a well-defined time, according to the data presented in Table 3. In order to avoid settling, the slurry was constantly stirred during all the experiments.

The AC performances were characterized by measuring the rate of BCG decolorization by adsorption.

Since one of its typical applications is the pH indicator, the BCG is highly sensitive to pH deviations. The pH increase from being acidic to basic leads to a color variation ranging from yellow to green and blue. The UV-Vis spectrum of BCG also varies with the pH change. BCG's acid and basic forms display an isosbestic point in their UV-Vis spectrum, around 515 nm [68, 76]. Zaggout [76] and Fassi et al. [68] show that at acidic and natural pH, the most intense band is at around 614 nm, while at basic pH, the most intense band is shifted to around 444 nm. The pH sensitivity of BCG, certified by the spectroscopic versatility, is highlighted in various literature reports. Many authors working with BCG reported different values of the reference band (Table 4). Some followed the band at 440 nm, while others tracked it at 614 nm.

During this study, the absorbance values at 412 nm (Figure 3(a)) were used to analyze the process course. BCG concentration was calculated from an absorbance versus concentration calibration curve with an R^2 value of 0.99677 (Figure 3(b)). It is worth mentioning that the calibration curve failed from linearity when parallel measurements were done at 617 nm (results not shown).

The efficiency of BCG decolorization η (%) was calculated using the following equation:

$$\eta\,[\%] = \frac{\mathrm{BCG}^0 - \mathrm{BCG}^t}{\mathrm{BCG}^0}, \quad (1)$$

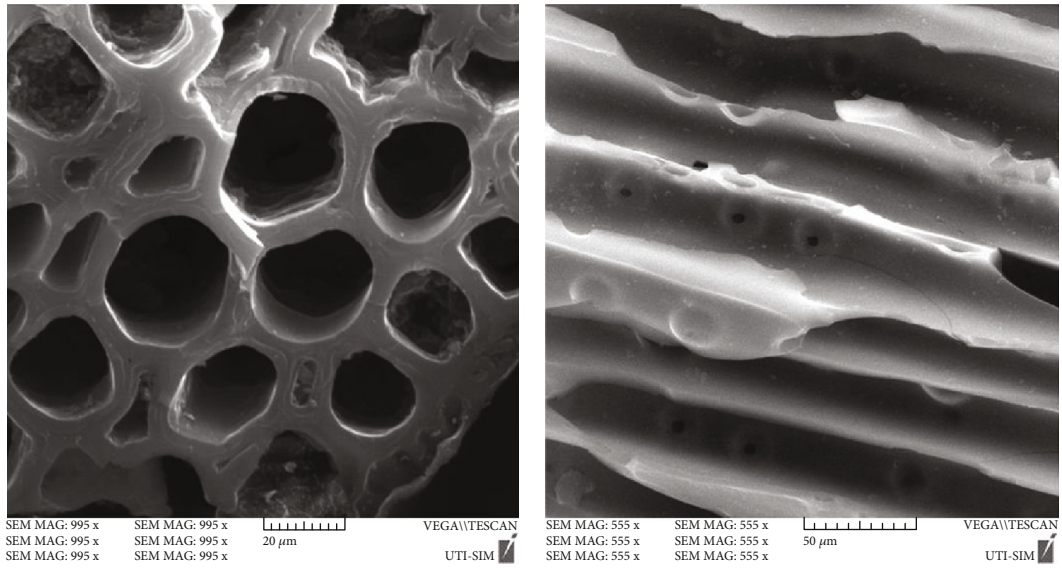

(a) (b)

Figure 2: SEM images of the commercial AC: pore size, shape, and alignment.

Table 2: Designated variables and their variation range for BCG decolorization with active carbon.

Independent variables	Measure units	Range		Symbol
		From	To	
BCG concentration	g/L	0.009	0.045	BCG
Adsorbent amount	g/L	0.5	3	AA
Contact time	min	60	240	CT

where BCG^0 and BCG^t are the BCG (g/L) concentrations at the time $t = 0$ and at the time $t = t$.

2.5. Bacterial Foraging Optimization. BFO is an optimization technique inspired by the foraging behavior of *E. coli* bacteria. In order to provide solutions to a specific problem, it simulates the evolution of a series of potential solutions using a set of specific mechanisms that include chemotaxis, reproduction, elimination, and dispersal (Figure 4).

All these steps are repeated until a stop criterion is reached. For the standard BFO, this stop criterion is represented by the number of dispersal steps (N_{ed}). In this work, the stop criterion combines two criteria, and the algorithm stops when one of them becomes true. These criteria are (i) the number of dispersal steps and (ii) the number of function evaluations (FEs). The reason for this modification relies on the fact that FEs can be relatively easily set as a stop criterion for almost all bioinspired metaheuristics and can be further used for comparison purposes, while the number of internal repetitions an algorithm performs does not correctly show the computational resources consumed versus the efficiency of the solution provided.

As can be observed from Figure 3, there is a close interconnection between the steps of the algorithm. The most iterated step is chemotaxis, which represents the movement of bacteria from food-scarce areas to affluent areas through swimming and tumbling. This is done by all bacteria (which, for the sake of simplicity, will be further referred to as individuals, and the colony of bacteria will be referred to as population) several times indicated by the N_c parameter. In the BFO algorithm, the mechanism used for food searching is associated with the repellent-attraction biological principle [79].

In the reproduction step, the individuals are sorted based on their fitness (a function that measures the individual's fitting to the environment). After that, the best individuals reproduce, while the worst ones are removed. This is performed N_{re} times, during which the population will be centered on several clusters and the overall diversity reduced. Therefore, to simulate the migration of bacteria into a new environment, with a probability indicated by a parameter (p_{ed}), some individuals are randomly replaced with new ones (the elimination-dispersal step).

In the initial BFO, p_{ed} has a fixed value; therefore, as the population evolves, the probability of replacing good individuals is the same as replacing worse individuals. As a result, individuals located in the vicinity of the global optimum can be replaced with individuals far from the optimum. Thus, potentially good solutions to the problem at hand can be lost. In order to avoid this aspect, in this work, p_{ed} is modified adaptively (equation (2)). This modification represents the main idea of the iBFO variant used in this work.

$$p_{ed} = \begin{cases} \dfrac{\text{fit}_{min} + \text{fit}_{avg}}{\text{fit}_{max} + \text{fit}_{min}}, & \text{if the objective is fitness minimization,} \\ \dfrac{\text{fit}_{max} - \text{fit}_{avg}}{\text{fit}_{max} - \text{fit}_{min}}, & \text{if the objective is fitness maximization,} \end{cases} \quad (2)$$

Table 3: Designated variables and their variation range for BCG decolorization with active carbon.

No.	Type[1]	Input variables						Response η (%)
		BCG (g/L)		AA (g/L)		CT (min)		
		Real	Coded[2]	Real	Coded[2]	Real	Coded[2]	
1	O1	0.045	1	3.006	1	240	1	27.96
2	O2	0.009	1	3.004	−1	240	1	31.94
3	O3	0.045	1	3.002	1	60	−1	21.54
4	O4	0.009	1	3.002	−1	60	−1	28.95
5	O5	0.045	−1	0.506	1	240	1	13.37
6	O6	0.009	−1	0.506	−1	240	1	23.77
7	O7	0.045	−1	0.5	1	60	−1	9.23
8	O8	0.009	−1	0.501	−1	60	−1	32.21
9	S1	0.049	0	1.754	α	150	0	18.27
10	S2	0.0051	0	1.752	$-\alpha$	150	0	44.60
11	S3	0.027	0	1.753	0	259.35	α	28.31
12	S4	0.027	0	1.757	0	40.65	$-\alpha$	16.33
13	S5	0.027	α	3.27	0	150	0	21.23
14	S6	0.027	$-\alpha$	0.23	0	150	0	12.16
15	C1	0.027	0	1.752	0	150	0	21.50
16	C2	0.027	0	1.752	0	150	0	21.59
17	C3	0.027	0	1.75	0	150	0	22.50
18	C4	0.027	0	1.754	0	150	0	24.32

[1]O = orthogonal design points; S = axial or star points; C = center points. [2]-1 = low value, 1 = high value, 0 = center value, and $-\alpha$, α = star point value.

Table 4: Literature reported BCG reference bands.

Authors	Tracked band (nm)	Ref.
Ghaedi et al.; this work	412	[62]; this work
Özdemir et al.	424	[63]
Salmalian et al.	430	[65]
Khan et al.	438	[73]
Bhanuprakash and Belagali; Murmu et al.; Shokrollahi et al.	442	[60, 64, 77]
Fassi et al.; Fassi et al.	444	[68, 69]
Palazzolo et al.	404 and 617	[78]
Bai et al.	613	[66]
Liu et al.	614	[61]
Chaleshtori et al.	616	[70]
Palazzolo et al.	617	[78]
Ying et al.	620	[71]
Torğut and Demirelli	623	[67]

where fit_{min}, fit_{max}, and fit_{avg} are the minimum, maximum, and average of the fitness of all individuals in the population.

In order to determine the optimal conditions for the considered process, two models were considered: (i) the regression equations determined using the RSM-based approach and (ii) ANNs. In the second case, the ANNs, on their own, required a series of optimization to determine their best parameters. Thus, in this work, iBFO is applied to perform two optimization types: process and model optimization.

Regarding process optimization, the process parameters are evolved and then fed into the considered model to generate the necessary predictions. On the other hand, in the case of ANN optimization, the necessary ANN parameters are directly encoded into a vector containing real numbers and then fed into the iBFO. This encoding is necessary because iBFO cannot directly work with ANN structures. Even though in neuroevolution, both topology (structure and organization of the neurons) and training can be performed by the optimizer, in this work, iBFO performs only

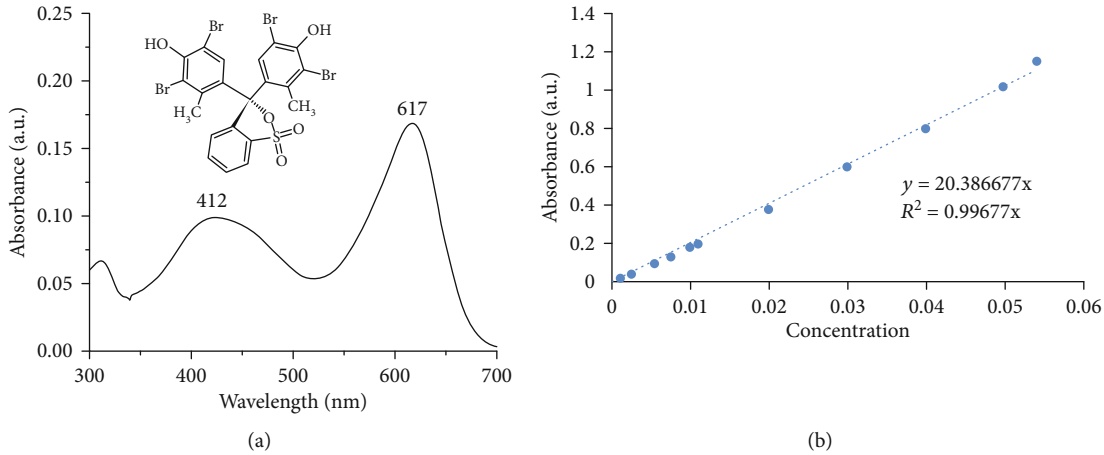

Figure 3: Chemical structure of BCG: (a) UV-Vis spectra and absorbance; (b) concentration calibration curve.

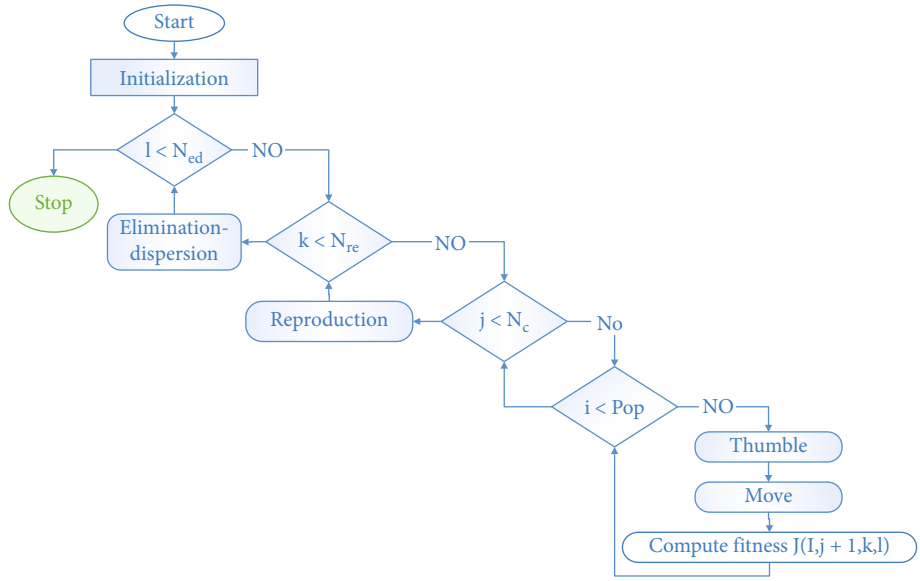

Figure 4: Schema of the BFO algorithm.

a topology determination. The training procedure is the standard approach used in the Keras framework for the ANN model implementation in combination with Adam, a stochastic optimizer based on scaled gradient updates. The type of model considered is sequential. The entire software implementation (iBFO and ANNs) was performed in Python.

3. Results and Discussions

3.1. Response Surface Method. The parameters that directly affect the efficiency of the decolorization process are BCG, AA, and CT, as presented in Table 2. In order to study the combined outcome of these three factors, experiments were performed, varying their values in carefully chosen intervals (Table 2), following a statistically designed experimental routine (Table 3). The experimental results were analyzed and interpreted using the MINITAB 17.1.0 software package. The full quadratic model obtained (equation (3)) had an R^2 of 90.34% and an adjusted R^2 of 79.47%.

$$\begin{aligned}\eta\,[\%] = {} & 42.85 - 1741 \cdot \mathrm{BCG} - 0.0236 \cdot \mathrm{CT} + 7.04 \cdot \mathrm{AA} \\ & + 17631 \cdot \mathrm{BCG}^2 - 0.000056 \cdot \mathrm{CT}^2 - 2.72 \cdot \mathrm{AA}^2 \\ & + 1.231 \cdot \mathrm{BCG} \cdot \mathrm{CT} + 122.1 \cdot \mathrm{BCG} \cdot \mathrm{AA} + 0.0154 \cdot \mathrm{CT} \cdot \mathrm{AA}.\end{aligned} \tag{3}$$

By setting one parameter at a constant value, preferable to the value in the middle of the designated interval of variation, three-dimensional plots (surface plots) were drawn as presented in Figures 5(a)–5(c).

Such exposure of the parameter variation allows the visualization of maximum and/or minimum points, which leads to accurate identification of the optimal values, highlighting the impact of the selected parameters on the decolorization efficiency.

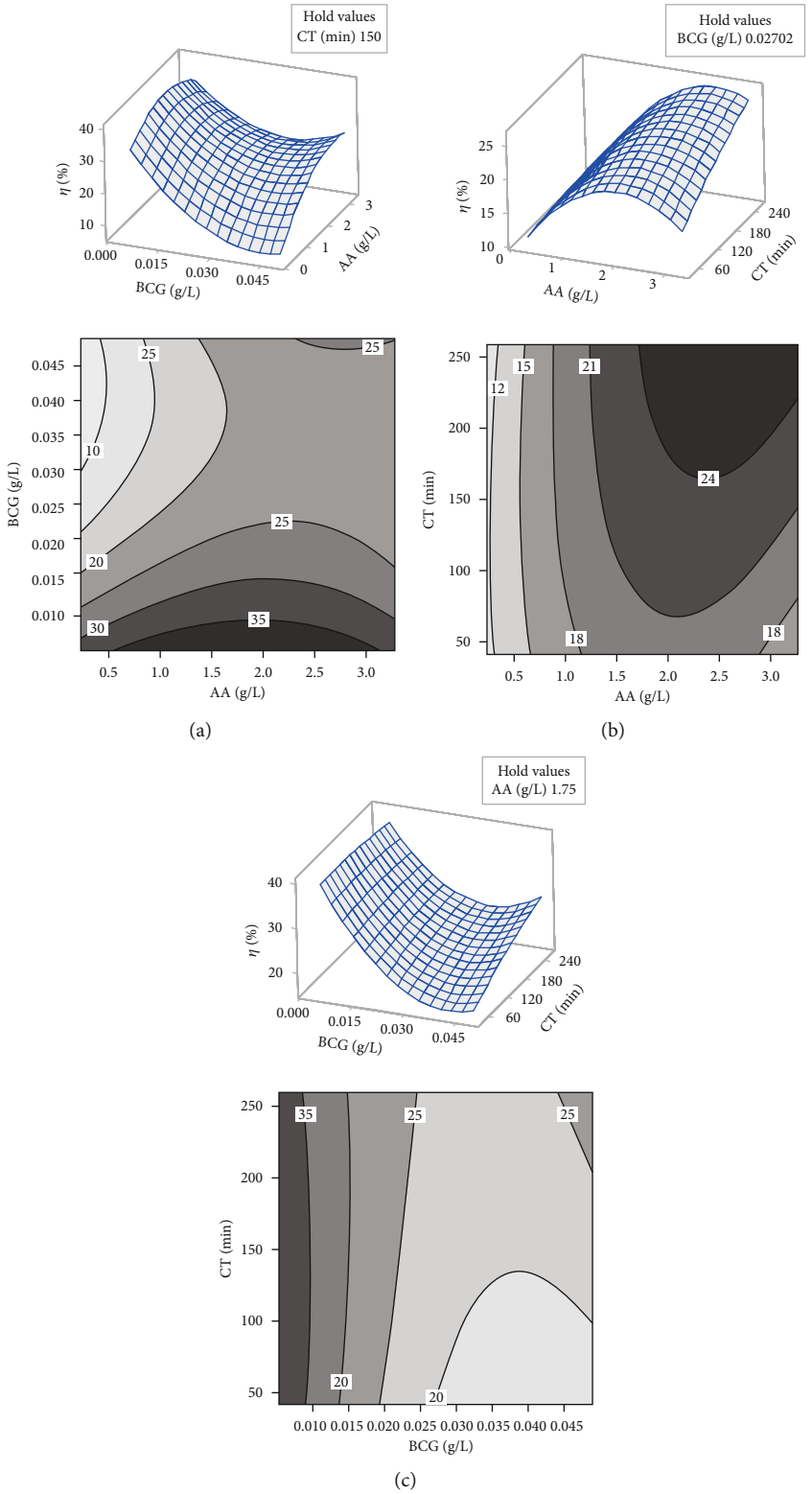

Figure 5: Surface and contour plots: (a) efficiency vs. BCG (g/L) and AA (g/L) at CT = 150 min; (b) efficiency vs. AA (g/L) and CT (min) at BCG = 0.02702 g/L; (c) efficiency vs. BCG (g/L) and CT (min) at AA = 1.75 g/L.

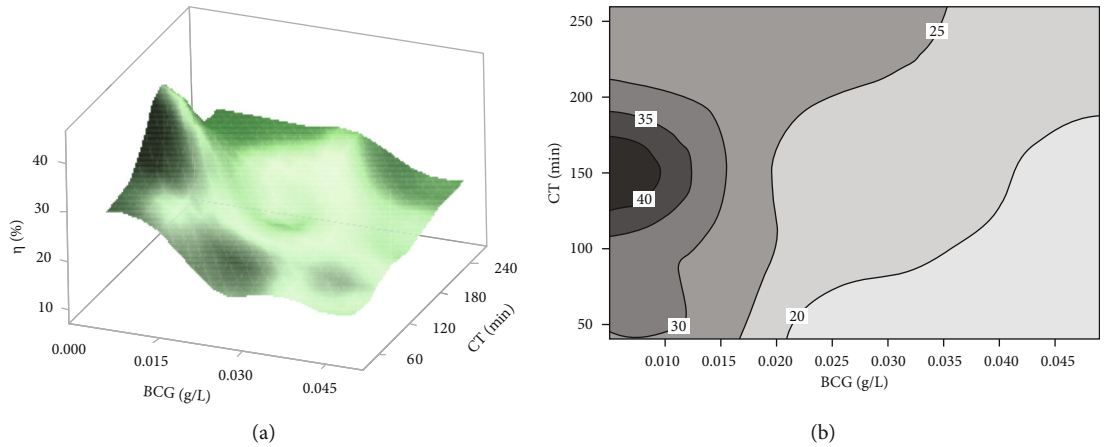

(a) (b)

Figure 6: (a) Three-dimensional response surface displaying the effects of BCG and CT on the process efficiency. (b) Two-dimensional contour plot showing the effects of BCG and CT on the process efficiency.

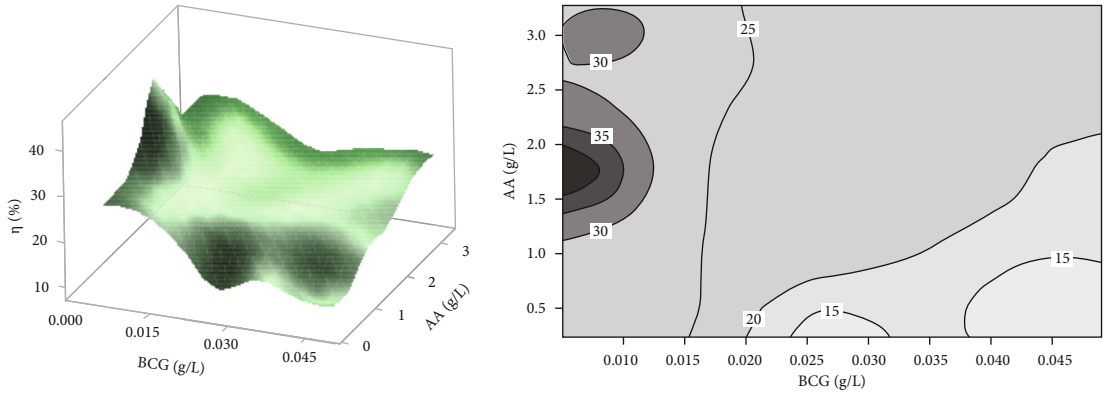

(a) (b)

Figure 7: (a) Three-dimensional response surface displaying the effects of BCG and AA on the process efficiency. (b) Two-dimensional contour plot showing the effects of BCG and AA on the process efficiency.

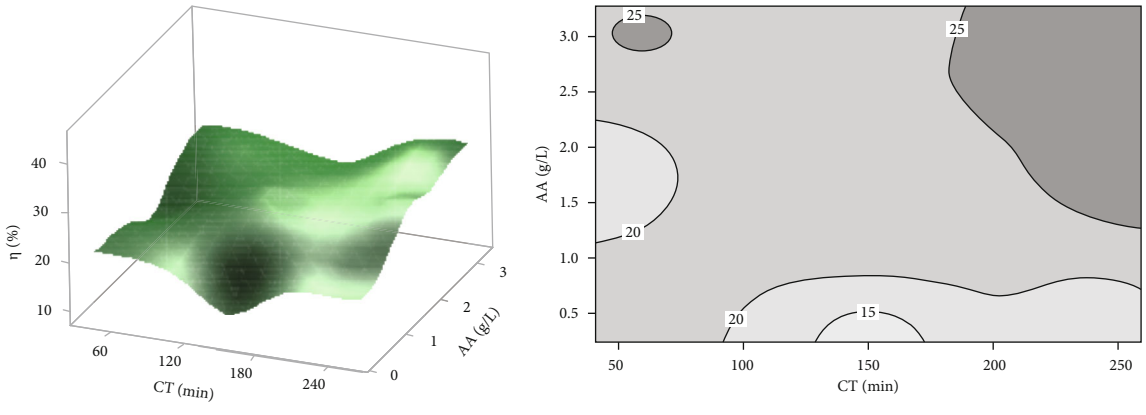

(a) (b)

Figure 8: (a) Three-dimensional response surface displaying the effects of CT and AA on the process efficiency. (b) Two-dimensional contour plot showing the effects of CT and AA on the process efficiency.

Table 5: Optimization results obtained with BFO and RSM for typical and extrapolation cases.

Case	Sol. no.	AA (g/L)	CT (min)	BCG (g/L)	η (%)
(i) Typical (-1,1 from DOE)*	1	1.683	81	0.010000	34.2
	2	1.830	235	0.010086	34.0
	3	1.632	122	0.010413	33.9
	4	1.819	151	0.010711	33.8
	5	1.948	216	0.011115	33.4
(ii) Extrapolation ($-\alpha, \alpha$ from DOE)*	6	1.844	197	0.005111	39.3
	7	2.112	212	0.005184	39.1
	8	2.018	99	0.007150	37.3
	9	1.485	123	0.007219	37.1
	10	1.162	79	0.007698	36.0

* $-\alpha$, -1, 0, 1, and α are the coding levels for the values from Table 3.

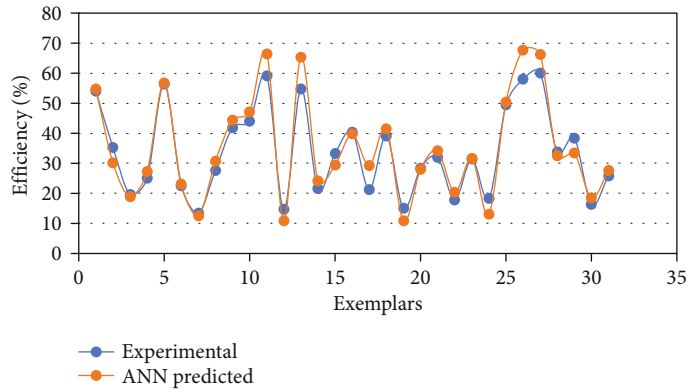

Figure 9: Evolution of the MSE in the training and validation phases for the best model obtained.

Table 6: Optimization results based on the ANN model.

Case	Sol. no.	AA (g/L)	CT (min)	BCG (g/L)	η (%)
(i) Model limits	1	0.110	4080	0.001730	99.9
	2	1.012	3862	0.001490	95.8
	3	1.188	1813	0.000330	93.0
	4	0.188	1737	0.000330	92.5
	5	2.771	3551	0.043100	92.3
(ii) (-1,1) from DOE*	6	1.777	237	0.009000	45.6
	7	1.685	235	0.009800	43.9
	8	1.687	227	0.011010	43.9
	9	1.795	238	0.009070	43.8
	10	1.353	155	0.027460	37.1
(iii) $(-\alpha, \alpha)$ from DOE*	11	1.844	197	0.005111	39.3
	12	2.112	212	0.005184	39.1
	13	2.243	202	0.006830	37.4
	14	1.485	123	0.007219	37.1
	15	1.162	79	0.007698	36.0

* $-\alpha$, -1, 0, 1, and α are the coding levels for the values from Table 3.

The 3D (three-dimensional) surface plots and contour plots were used to graphically describe decolorization efficiency at different values of the main process parameters. The interactive effect of bromocresol concentration and contact time for an adsorbent concentration of 1.75 g/L is illustrated in Figures 6(a) and 6(b). The active carbon performs better at lower BCG concentrations. The prolongation of contact time after reaching the equilibrium does not have positive outcomes towards decolorization efficiency.

The combined effect of AA and BCG after 150 min CT on the efficiency is depicted in Figures 7(a) and 7(b). It can be observed that the percentage of adsorbed BCG is increased with raising the adsorbent dosage especially at lower BCG values. The growing of the adsorbent amount besides a 2.5 g/L threshold does not improve the adsorption yield.

Finally, the evolution of the decolorization efficiency as a function of the contact time and the adsorbent amount is presented in Figure 8, where the interactive effect of these two parameters is studied at fixed values of BCG. As expected, raising the adsorbent amount and the contact time leads to an increase in BCG retention percentage.

According to the RSM method, the optimal values of the considered variables are BCG = 5.135 E − 03 g/L, AA = 1.58

Table 7: Comparison of several adsorbents' efficiency in decolorizing BCG.

Adsorbent	Considered process parameters	Optimization method	η (%)	Ref.
Acid-treated charcoal (ACT)	UV irradiation time, catalyst dosage, recycled catalyst dosage.	—	16.85	[73]
Co-adsorbed ACT			40.5	
AC derived from rice husk	Contact time, temperature, adsorbent dosage, pH, and initial concentration	—	93	[72]
Chitin nanofibers	Contact time, temperature, adsorbent dosage, pH, and initial concentration	IBM SPSS statistics; one-way ANOVA	92.75	[65]
Zeolitic imidazolate framework (ZIF-11)	pH, stirring speed, contact time, temperature	—	89	[80]
Almond husk	pH, adsorbent dosage, contact time, and initial and final concentration	—	97.5	[77]
Rice straw biochar	Biochar, pyrolysis temperature, solution pH, biochar dosage, initial dye concentration, and contact time	—	80	[81]
Rice husk biochar			50	
Activated biosorbent Phragmites karka	pH, agitation speed, contact time, biosorbent dosage, initial dye concentration, temperature	—	99.99	[64]
Fe_3O_4/MIL-88A nanocomposite	Contact time, adsorbent dosage, initial concentration	—	70	[82]
Commercial active carbon	Contact time, adsorbent dosage, initial concentration	Differential evolution	99.83	[75]
		RSM	97.77	
		Differential search	99.99	
Commercial active carbon	Contact time, adsorbent dosage, initial concentration	RSM	39.3	This work
		iBFO	>99	

g/L, and CT = 62.74 min that lead to 39.92% process efficiency.

As observed, there is a complex interdependency between the process parameters. Therefore, the standard analysis of the variation of efficiency considering two parameters at once does not provide a complete picture regarding the output parameters' lowest or highest surface points. Furthermore, since the RSM performs the optimization by setting some parameters fixed and varying only a few (usually just one parameter), the search space is not efficiently explored, and there is the possibility that other solutions can be found. Thus, iBFO was applied to perform an exhaustive search and identify promising high-efficiency regions.

The optimal results attained with this method (39.92%) are comparable to those reported in other studies focusing on the decolorization of bromocresol green with different types of active carbon. For example, in [73], the maximum efficiency of active charcoal from pine cones doped with Co was 41.86%.

3.2. Bacterial Foraging Optimization. Two cases were considered for process optimization using bacterial foraging optimization: (i) the statistical model determined using RSM and (ii) an ANN model. However, the determination of the ANN model is, in its turn, an optimization problem, and thus, iBFO was also applied for model optimization. In both the model and process optimization, the settings for the iBFO parameters were the same: $N_c = 20$, $N_s = 5$, $N_{re} = 8$, $N_{ed} = 20$, and the initial value for $p_{ed} = 0.25$.

3.2.1. RSM-Based Optimization. Using the regression model determined by the RMS approach (equation (3)), iBFO was applied to determine if additional optimal points could be found by thoroughly searching the search space indicated by the process parameters. To this means, the maximum process efficiency was identified based on AA, CT, and BCG.

As iBFO is flexible and permits an easy alteration of the intervals for the process parameters, multiple optimization cases were considered: (i) typical (when the minimum and maximum values for the independent variables are identical to the experiments, coded -1 and 1 from the DOE planning) and (ii) extrapolation (where the limits are set to $-\alpha$ and α from the DOE planning). Thus, in each considered case, ten runs were performed. From the multitude of solutions (from the vicinity of the optimum) provided by iBFO, for each case, Table 5 presents the best five combinations of parameters that optimize the process.

As observed in Table 5, the iBFO algorithm provided various solutions indicating a high capability of exploring the search space and finding promising areas. Depending on the specific requirements at a given time, the end user or the process manager can select a different optimization solution. Compared to the RSM approach, the iBFO, in combination with the statistical model, provided results similar in terms of efficiency. However, iBFO generated multiple solutions in the vicinity of the optimum, indicating that the interaction between parameters is complex and that different combinations of parameters lead to the same efficiency.

3.2.2. ANN-Based Optimization. In this case, the iBFO role is to determine the optimal topology that best fits the

considered process. The sequential ANNs considered in this work are trained using a supervised approach, and thus, the experimental data describing the process is used for hyperparameter tuning. However, as the number of experiments resulting from the standard DOE planning is relatively small, a series of random experiments were performed to increase the number of points that can be included in the training/testing phase. As a result, the efficiency was measured for a more extended period compared with the DOE plan. Thus, compared with the RSM strategy, the ANN model can predict without extrapolating a higher number of parameter combinations.

In order to perform the model determination, the standard data processing techniques used in the machine learning area were applied: (i) data normalization, (ii) data randomization, and (ii) data splitting. For data normalization, all the experimental points were normalized in the [-1,1] interval to ensure that no specific process parameter significantly influences the model based on the order of magnitude for its values. After that, to ensure that training is not performed on a subgroup of points, the data is randomly assigned to one of the phases: training/testing. The percentage of training data is 75%, and 25% is for testing.

After data processing, iBFO was applied to determine the best-suited model. This suitability is measured by the fitness function, which in the case of ANN determination is represented by the Mean Squared Error (MSE) in the training phase. The elements evolved by iBFO are strictly related to topology (hidden layers and neurons in each hidden layer). As the current iBFO version works with a population of fixed dimension, which for the current case corresponds to a limit on the number of hidden layers, based on a series of preliminary analyses, it was set to 5. Furthermore, the activation function for each neuron from the hidden layer is set to ReLU, while the activation function for the output layer is linear. Finally, in order to train each identified topology, the Adam optimizer was considered.

The best model obtained had two hidden layers with 33 and 22 neurons, respectively. The MSE was 16.14 in the training phase and 26.7 in the testing phase. The average absolute error and the correlation were 9.14% and 0.962 for training and 10.73% and 0.961 for testing. A comparison between the experimental and predicted values for the testing data is presented in Figure 9. As it can be observed, for most exemplars, the differences are relatively small, indicating the model's capability to capture the process efficiently.

iBFO and the determined ANN were then utilized to optimize the process. Table 6 presents the best five solutions provided by the model. In this case, two situations were considered: (i) when the limits for the search are the ones obtained through the supplementary experiments performed to expand the dataset, (ii) when the limits are set as in the DOE approach (-1,1), and (iii) when the limits are set to $(-\alpha, \alpha)$.

As seen in Table 6, the results considering the extended limits allow the identification of conditions that lead to ~100% efficiency. Regarding cases where the (-1,1) interval was considered, the solutions provided with the ANN-based model have a higher efficiency than those obtained with the RSM-based model. On the other hand, for the $(-\alpha, \alpha)$, the solutions provided had a similar efficiency. Therefore, the results obtained in this case are similar to those presented in the literature. For example, in [72], for an active carbon produced from rice husks, the maximum efficiency was 93%.

Overall, the results obtained with iBFO when using both the RSM and the ANN-based models indicate that the optimizer can explore the search space and identify distinct solutions in the vicinity of the optimum. Furthermore, this variety can support a large area of use cases where a specific parameter can be limited within the desired interval (considering a maximum efficiency and a minimization of consumed resources).

3.3. Comparison with Other Adsorbents. Several adsorbents have been used for BCG decolorization/removal from wastewater. Most of them are active carbons/charcoals prepared from various lignocellulosic biomass. Chitins, polymers, and various nanocomposites were also used, as presented in Table 7.

Most authors report the direct influence of individual process parameters on decolorization efficacy, such as adsorbent dosage, contact time, initial BCG concentration, pH, and temperature. However, only a few show optimization studies that report the conjugate influence of the process parameters and classify them in order of their significance for the process.

4. Conclusions

This study applied various modeling and optimization strategies to BCG decolorization on commercial activated carbon with the scope of demonstrating that the application of new approaches from the artificial intelligence area can provide optimal solutions. The methodologies included conventional (RSM) and nonconventional artificial intelligence methodologies (ANNs and a modified version of bacterial foraging optimization). iBFO was utilized as an optimizer for the model and process, with its adaptability and capabilities substantiating the favorable results obtained.

First, in order to consume the minimum resources (time, chemicals, etc.), the DOE methodology was applied to program a minimal number of statistically relevant experiments. Then, the most used strategy encountered in literature (RSM) was applied. Using the MINITAB 17.1.0 software suite, the findings were analyzed and interpreted and a statistical model was determined and then used for process optimization, with the maximum efficiency obtained being 39.92% at BCG = $5.135E-03$ g/L, AA = 1.58 g/L, and CT = 62.74 min. Compared with the experimental data obtained for the $[-\alpha, \alpha]$ DOE limits, this optimal value is close, but lower. This can be explained by the RSM-based model error ($R^2 = 90.34\%$). These results point out that this approach is not able to find better solutions.

To further test if the issue of not finding better solutions than the experimental data is related to the optimization strategy or to the model, the statistical model was applied in combination with iBFO. While the maximum efficiency

obtained was similar when using the same statistic model, iBFO could find multiple distinct combinations of parameters that lead to the same efficiency. This proved the capability of the optimizer to explore the search space efficiently and identify the regions with promising potential (local and global minima). These results also pointed out that within the considered DOE limits of $[-\alpha, \alpha]$, a higher efficiency could not be obtained.

Thus, a series of additional random experiments were performed and, together with the DOE plan, were used to determine an ANN model. First, its optimized topology (2 hidden layers with 33 neurons in the first one and 22 neurons in the second one) was identified using the iBFO approach. Then, it is applied to optimize the process considering different limitations for parameters. In this case, conditions that lead to >99% efficiency were identified, proving that even the classical processes can be further improved when good strategies are applied.

The strategy of starting with standard approaches and then when they fail to provide improved solutions to replace them with novel strategies from the area of artificial intelligence demonstrated that process modeling and optimization are not a straightforward fit-all approach and that there are cases where multiple variants must be tested before reaching an acceptable solution. The good results of the current case study pave the way for the advanced optimization of other types of processes, with a significant economic and industrial impact.

Data Availability

The data supporting the reported results is presented in the manuscript.

Conflicts of Interest

The authors highlight that they have no known competing financial interests or personal relationships that could have appeared to influence the work reported in this study.

Authors' Contributions

The authors are responsible for correctness of the statements provided in the manuscript.

Acknowledgments

This work was supported by "Program 4: Fundamental and frontier research—Exploratory research projects" financed by UEFISCDI (project no. PCE 58/2021).

References

[1] A. Abel, *The history of dyes and pigments: from natural dyes to high performance pigments, in Colour Design*, J. Best, Ed., Woodhead Publishing, 2nd edition, 2012.

[2] A. Gürses, M. Açıkyıldız, K. Güneş et al., "Classification of dye and pigments," in *Dyes and Pigments*, pp. 31–45, Springer International Publishing, Cham, 2016.

[3] L. P. Lingamdinne, S. Lee, J. S. Choi, V. R. Lebaka, V. R. P. Durbaka, and J. R. Koduru, "Potential of the magnetic hollow sphere nanocomposite (graphene oxide-gadolinium oxide) for arsenic removal from real field water and antimicrobial applications," *Journal of Hazardous Materials*, vol. 402, article 123882, 2021.

[4] R. I. Alsantali, Q. A. Raja, A. Y. A. Alzahrani et al., "Miscellaneous azo dyes: a comprehensive review on recent advancements in biological and industrial applications," *Dyes and Pigments*, vol. 199, article 110050, 2022.

[5] L. D. Ardila-Leal, R. A. Poutou-Piñales, A. M. Pedroza-Rodríguez, and B. E. Quevedo-Hidalgo, "A brief history of colour, the environmental impact of synthetic dyes and removal by using laccases," *Molecules*, vol. 26, no. 13, p. 3813, 2021.

[6] R. M. El-Shishtawy, "Functional dyes, and some hi-tech applications," *International Journal of Photoenergy*, vol. 2009, Article ID 434897, 21 pages, 2009.

[7] S. Benkhaya, S. M'rabet, and A. El Harfi, "A review on classifications, recent synthesis and applications of textile dyes," *Inorganic Chemistry Communications*, vol. 115, article 107891, 2020.

[8] S. Benkhaya, S. M'rabet, H. Lgaz, A. el Bachiri, and A. el Harfi, "Dyes: classification, pollution, and environmental effects," in *Dye Biodegradation, Mechanisms and Techniques: Recent Advances*, S. S. Muthu and A. Khadir, Eds., pp. 1–50, Springer, Singapore, 2022.

[9] S. H. Hashemi and M. Kaykhaii, "Azo dyes: sources, occurrence, toxicity, sampling, analysis, and their removal methods," in *Emerging Freshwater Pollutants*, T. Dalu and N. T. Tavengwa, Eds., pp. 267–287, Elsevier, 2022.

[10] A. Gürses, K. Güneş, and E. Şahin, "Removal of dyes and pigments from industrial effluents," in *Green Chemistry and Water Remediation: Research and Applications*, S. K. Sharma, Ed., pp. 135–187, Elsevier, 2021.

[11] R. Al-Tohamy, S. S. Ali, F. Li et al., "A critical review on the treatment of dye-containing wastewater: ecotoxicological and health concerns of textile dyes and possible remediation approaches for environmental safety," *Ecotoxicology and Environmental Safety*, vol. 231, article 113160, 2022.

[12] O. J. Hao, H. Kim, and P.-C. Chiang, "Decolorization of wastewater," *Critical Reviews in Environmental Science and Technology*, vol. 30, no. 4, pp. 449–505, 2000.

[13] Y. Anjaneyulu, N. Sreedhara Chary, and D. Samuel Suman Raj, "Decolourization of industrial effluents – available methods and emerging technologies – a review," *Reviews in Environmental Science and Bio/Technology*, vol. 4, no. 4, pp. 245–273, 2005.

[14] S. Samsami, M. Mohamadizaniani, M. H. Sarrafzadeh, E. R. Rene, and M. Firoozbahr, "Recent advances in the treatment of dye-containing wastewater from textile industries: overview and perspectives," *Process Safety and Environmental Protection*, vol. 143, pp. 138–163, 2020.

[15] M. C. Collivignarelli, A. Abbà, M. Carnevale Miino, and S. Damiani, "Treatments for color removal from wastewater: state of the art," *Journal of Environmental Management*, vol. 236, pp. 727–745, 2019.

[16] A. K. Verma, R. R. Dash, and P. Bhunia, "A review on chemical coagulation/flocculation technologies for removal of colour from textile wastewaters," *Journal of Environmental Management*, vol. 93, no. 1, pp. 154–168, 2012.

[17] J. Behin, N. Farhadian, M. Ahmadi, and M. Parvizi, "Ozone assisted electrocoagulation in a rectangular internal-loop airlift reactor: application to decolorization of acid dye," *Journal of Water Process Engineering*, vol. 8, pp. 171–178, 2015.

[18] A. H. Konsowa, M. E. Ossman, Y. Chen, and J. C. Crittenden, "Decolorization of industrial wastewater by ozonation followed by adsorption on activated carbon," *Journal of Hazardous Materials*, vol. 176, no. 1-3, pp. 181–185, 2010.

[19] D. Shahbazi, S. A. Mousavi, and D. Nayeri, "Low-cost activated carbon: characterization, decolorization, modeling, optimization and kinetics," *International Journal of Environmental Science and Technology*, vol. 17, no. 9, pp. 3935–3946, 2020.

[20] B. Beigzadeh, M. Bahrami, M. J. Amiri, and M. R. Mahmoudi, "A new approach in adsorption modeling using random forest regression, Bayesian multiple linear regression, and multiple linear regression: 2,4-D adsorption by a green adsorbent," *Water Science and Technology*, vol. 82, no. 8, pp. 1586–1602, 2020.

[21] M. Bahrami, M. J. Amiri, and F. Bagheri, "Optimization of the lead removal from aqueous solution using two starch based adsorbents: design of experiments using response surface methodology (RSM)," *Journal of Environmental Chemical Engineering*, vol. 7, no. 1, article 102793, 2019.

[22] J. L. Wang and L. J. Xu, "Advanced oxidation processes for wastewater treatment: formation of hydroxyl radical and application," *Critical Reviews in Environmental Science and Technology*, vol. 42, no. 3, pp. 251–325, 2012.

[23] A. S. Powar, A. Perwuelz, N. Behary, L. Hoang, and T. Aussenac, "Application of ozone treatment for the decolorization of the reactive-dyed fabrics in a pilot-scale process—optimization through response surface methodology," *Sustainability*, vol. 12, no. 2, pp. 471–485, 2020.

[24] S. Khameneh Asl, B. Mohammadi, and A. Khataee, "Optimization of anodizing parameters on photo decolorization of textile dye solution using N-doped titanium nanotubes with response surface methodology," *Asian Journal of Green Chemistry*, vol. 4, pp. 258–275, 2020.

[25] R. G. Saratale, G. D. Saratale, J. S. Chang, and S. P. Govindwar, "Decolorization and biodegradation of reactive dyes and dye wastewater by a developed bacterial consortium," *Biodegradation*, vol. 21, no. 6, pp. 999–1015, 2010.

[26] T. Arfin, N. Varshney, and B. Singh, "Ionic liquid modified activated carbon for the treatment of textile wastewater," in *Green Materials for Wastewater Treatment*, pp. 257–275, Springer, 2020.

[27] D. M. Lewis, "Coloration in the next century," *Review of Progress in Coloration and Related Topics*, vol. 29, no. 1, pp. 23–28, 1999.

[28] A. Venkataraman, L. Babu, and K. Aravamudan, "Unified, simple and decentralized treatment process for synthetic and real-time dye contaminated wastewaters," *Journal of Hazardous Materials*, vol. 423, no. Part B, article 127059, 2022.

[29] A. Singh, D. B. Pal, A. Mohammad et al., "Biological remediation technologies for dyes and heavy metals in wastewater treatment: new insight," *Bioresource Technology*, vol. 343, article 126154, 2022.

[30] C. Zampeta, K. Bertaki, I. E. Triantaphyllidou, Z. Frontistis, P. G. Koutsoukos, and D. V. Vayenas, "Pilot-scale hybrid system combining hydrodynamic cavitation and sedimentation for the decolorization of industrial inks and printing ink wastewater," *Journal of Environmental Management*, vol. 302, article 114108, 2022.

[31] V. S. Hakke, M. M. Seepana, S. H. Sonawane, A. K. Kola, and R. Vooradi, "Hybrid treatment technologies for the treatment of industrial wastewater," in *Water Pollution and Remediation: Heavy Metals, Inamuddin*, M. I. Ahamed and E. Lichtfouse, Eds., pp. 211–241, Springer International Publishing, Cham, 2021.

[32] A. Dulov, N. Dulova, and M. Trapido, "Combined physicochemical treatment of textile and mixed industrial wastewater," *Ozone: Science & Engineering*, vol. 33, no. 4, pp. 285–293, 2011.

[33] X.-J. Ma and H.-L. Xia, "Treatment of water-based printing ink wastewater by Fenton process combined with coagulation," *Journal of Hazardous Materials*, vol. 162, no. 1, pp. 386–390, 2009.

[34] M. T. Nechita, G. D. Suditu, A. C. Puițel, and E. N. Drăgoi, "Differential evolution-based optimization of corn stalks black liquor decolorization using active carbon and TiO_2/UV," *Scientific Reports*, vol. 11, no. 1, pp. 1–12, 2021.

[35] G. Alam, I. Ihsanullah, M. Naushad, and M. Sillanpää, "Applications of artificial intelligence in water treatment for optimization and automation of adsorption processes: recent advances and prospects," *Chemical Engineering Journal*, vol. 427, article 130011, 2022.

[36] M. S. Secula, G. D. Suditu, I. Poulios, C. Cojocaru, and I. Cretescu, "Response surface optimization of the photocatalytic decolorization of a simulated dyestuff effluent," *Chemical Engineering Journal*, vol. 141, no. 1-3, pp. 18–26, 2008.

[37] A. I. Atomi, G. D. Suditu, A. C. Puițel, and M. T. Nechita, "Experimental study on TiO_2 promoted photo-degradation of methylene blue," *Bulletin of Romanian Chemical Engineering Society*, vol. 5, no. 1, pp. 68–74, 2018.

[38] A. Azari, M. Yeganeh, M. Gholami, and M. Salari, "The superior adsorption capacity of 2,4-dinitrophenol under ultrasound-assisted magnetic adsorption system: modeling and process optimization by central composite design," *Journal of Hazardous Materials*, vol. 418, article 126348, 2021.

[39] G. E. Box and J. S. Hunter, "Multi-factor experimental designs for exploring response surfaces," *The Annals of Mathematical Statistics*, vol. 28, no. 1, pp. 195–241, 1957.

[40] R. H. Myers, D. C. Montgomery, and C. M. Anderson-Cook, *Response surface methodology: process and product optimization using designed experiments*, John Wiley & Sons, 2016.

[41] A. I. Khuri and S. Mukhopadhyay, "Response surface methodology," *WIREs Computational Statistics*, vol. 2, no. 2, pp. 128–149, 2010.

[42] M. Y. Badi, A. Esrafili, H. Pasalari et al., "Degradation of dimethyl phthalate using persulfate activated by UV and ferrous ions: optimizing operational parameters mechanism and pathway," *Journal of Environmental Health Science and Engineering*, vol. 17, no. 2, pp. 685–700, 2019.

[43] A. Azari, M. H. Mahmoudian, M. H. Niari et al., "Rapid and efficient ultrasonic assisted adsorption of diethyl phthalate onto $Fe^{II}Fe_2^{III}O_4$@GO: ANN-GA and RSM-DF modeling, isotherm, kinetic and mechanism study," *Microchemical Journal*, vol. 150, article 104144, 2019.

[44] A. M. Ghaedi and A. Vafaei, "Applications of artificial neural networks for adsorption removal of dyes from aqueous solution: a review," *Advances in Colloid and Interface Science*, vol. 245, pp. 20–39, 2017.

[45] D. I. Fertu, E. N. Dragoi, L. Bulgariu, S. Curteanu, and M. Gavrilescu, "Modeling the biosorption process of heavy

metal ions on soybean-based low-cost biosorbents using artificial neural networks," *Processes*, vol. 10, no. 3, 2022.

[46] H. Faris, S. Mirjalili, and I. Aljarah, "Automatic selection of hidden neurons and weights in neural networks using grey wolf optimizer based on a hybrid encoding scheme," *International Journal of Machine Learning and Cybernetics*, vol. 10, no. 10, pp. 2901–2920, 2019.

[47] A. Tealab, "Time series forecasting using artificial neural networks methodologies: a systematic review," *Future Computing and Informatics Journal*, vol. 3, no. 2, pp. 334–340, 2018.

[48] K. M. Passino, "Biomimicry of bacterial foraging for distributed optimization and control," *IEEE Control Systems Magazine*, vol. 22, no. 3, pp. 52–67, 2002.

[49] E. N. Dragoi and V. Dafinescu, "Review of metaheuristics inspired from the animal kingdom," *Mathematics*, vol. 9, no. 18, p. 2335, 2021.

[50] B. Hernández-Ocana, E. Mezura-Montes, and P. Pozos-Parra, "A review of the bacterial foraging algorithm in constrained numerical optimization," in *2013 IEEE Congress on Evolutionary Computation*, pp. 2695–2702, Cancun, Mexico, 2013.

[51] C. Yang, J. Ji, J. Liu, and B. Yin, "Bacterial foraging optimization using novel chemotaxis and conjugation strategies," *Information Sciences*, vol. 363, pp. 72–95, 2016.

[52] C. Luo, X. Yin, and C. Ni, "A novel discrete bacterial foraging algorithm and its application," *The Journal of Communication*, vol. 10, no. 4, pp. 238–244, 2015.

[53] V. K. Gupta, "Application of low-cost adsorbents for dye removal - a review," *Journal of Environmental Management*, vol. 90, no. 8, pp. 2313–2342, 2009.

[54] D. Taylor, *Adsorbents, in Bleaching and Purifying Fats and Oils*, G. R. List, Ed., AOCS Press, 2nd edition, 2009.

[55] G. Crini, "Non-conventional low-cost adsorbents for dye removal: a review," *Bioresource Technology*, vol. 97, no. 9, pp. 1061–1085, 2006.

[56] M. M. Hassan and C. M. Carr, "A critical review on recent advancements of the removal of reactive dyes from dyehouse effluent by ion-exchange adsorbents," *Chemosphere*, vol. 209, pp. 201–219, 2018.

[57] A. Srinivasan and T. Viraraghavan, "Decolorization of dye wastewaters by biosorbents: a review," *Journal of Environmental Management*, vol. 91, no. 10, pp. 1915–1929, 2010.

[58] S. De Gisi, G. Lofrano, M. Grassi, and M. Notarnicola, "Characteristics and adsorption capacities of low-cost sorbents for wastewater treatment: a review," *Sustainable Materials and Technologies*, vol. 9, pp. 10–40, 2016.

[59] I. Haq, A. S. Kalamdhad, and A. Pandey, "Genotoxicity evaluation of paper industry wastewater prior and post-treatment with laccase producing Pseudomonas putida MTCC 7525," *Journal of Cleaner Production*, vol. 342, article 130981, 2022.

[60] A. Shokrollahi, A. Alizadeh, Z. Malekhosseini, and M. Ranjbar, "Removal of Bromocresol green from aqueous solution via adsorption on Ziziphus nummularia as a new, natural, and low-cost adsorbent: kinetic and thermodynamic study of removal process," *Journal of Chemical & Engineering Data*, vol. 56, no. 10, pp. 3738–3746, 2011.

[61] D. Liu, J. Yuan, J. Li, and G. Zhang, "Preparation of chitosan poly(methacrylate) composites for adsorption of Bromocresol green," *ACS Omega*, vol. 4, no. 7, pp. 12680–12686, 2019.

[62] M. Ghaedi, H. Khajesharifi, A. Hemmati Yadkuri, M. Roosta, R. Sahraei, and A. Daneshfar, "Cadmium hydroxide nanowire loaded on activated carbon as efficient adsorbent for removal of Bromocresol green," *Spectrochimica Acta Part A: Molecular and Biomolecular Spectroscopy*, vol. 86, pp. 62–68, 2012.

[63] M. Özdemir, Ö. Durmuş, Ö. Şahin, and C. Saka, "Removal of methylene blue, methyl violet, rhodamine B, alizarin red, and bromocresol green dyes from aqueous solutions on activated cotton stalks," *Desalination and Water Treatment*, vol. 57, no. 38, pp. 18038–18048, 2016.

[64] B. M. Murmu, S. S. Behera, S. Das, R. K. Mohapatra, B. K. Bindhani, and P. K. Parhi, "Extensive investigation on the study for the adsorption of Bromocresol green (BCG) dye using activated Phragmites karka," *Indian Journal of Chemical Technology*, vol. 25, pp. 409–420, 2018.

[65] E. Salmalian, H. Rezaei, and A. Shahbazi, "Removal of bromocresol green from aqueous solutions using chitin nanofibers," *Environmental Resources Research*, vol. 7, no. 2, pp. 79–86, 2019.

[66] H. Bai, P. He, J. Chen et al., "Electrocatalytic degradation of bromocresol green wastewater on Ti/SnO_2-RuO_2 electrode," *Water Science and Technology*, vol. 75, no. 1, pp. 220–227, 2017.

[67] G. Torğut and K. Demirelli, "Comparative adsorption of different dyes from aqueous solutions onto polymer prepared by ROP: kinetic, equilibrium and thermodynamic studies," *Arabian Journal for Science and Engineering*, vol. 43, no. 7, pp. 3503–3514, 2018.

[68] S. Fassi, I. Bousnoubra, T. Sehili, and K. Djebbar, "Degradation of "bromocresol green"by direct UV photolysis, acetone/UV and advanced oxidation processes (AOP's) in homogeneous solution (H2O2/UV, S2O8 2-/UV). Comparative study," *Journal of Materials and Environmental Science*, vol. 3, no. 4, pp. 732–743, 2012.

[69] S. Fassi, K. Djebbar, I. Bousnoubra, H. Chenini, and T. Sehili, "Oxidation of bromocresol green by different advanced oxidation processes: Fenton, Fenton-like, photo-Fenton, photo-Fenton-like and solar light. Comparative study," *Desalination and Water Treatment*, vol. 52, no. 25-27, pp. 4982–4989, 2014.

[70] M. Z. Chaleshtori, M. Hosseini, R. Edalatpour, S. M. S. Masud, and R. R. Chianelli, "New porous titanium-niobium oxide for photocatalytic degradation of bromocresol green dye in aqueous solution," *Materials Research Bulletin*, vol. 48, no. 10, pp. 3961–3967, 2013.

[71] Y. L. Ying, S. Y. Pung, M. T. Ong, and Y. F. Pung, "A comparison study between ZnO nanorods and WO_3/ZnO nanorods in bromocresol green dye removal," *Solid State Phenomena*, vol. 264, pp. 87–90, 2017.

[72] O. C. Elijah, O. N. Collins, O. C. Obumneme, and N. B. Jessica, "Application of modified agricultural waste in the adsorption of bromocresol green dye," *Asian Journal of Chemical Science*, vol. 7, no. 1, pp. 15–24, 2020.

[73] I. Khan, N. U. Rahman, A. Ali, and K. Saeed, "Adsorption of cobalt onto activated charcoal and its utilization for decolorization of bromocresol green dye," *Bulgarian Chemical Communications*, vol. 51, no. 4, pp. 488–493, 2019.

[74] M. S. Secula, B. Cagnon, I. Cretescu, M. Diaconu, and S. Petrescu, "Removal of an acid dye from aqueous solutions by adsorption on a commercial granular activated carbon: equilibrium, kinetic and thermodynamic study," *Scientific Study & Research. Chemistry & Chemical Engineering, Biotechnology, Food Industry*, vol. 12, no. 4, pp. 307–322, 2011.

[75] E. N. Dragoi, M. T. Nechita, and G. D. Suditu, "Bromocresol green adsorption optimization using bio-inspired

metaheuristic optimizers," in *Achievements and Perspectives of Modern Chemistry*, pp. 154–154, Chişinău, Moldova, 2019.

[76] F. R. Zaggout, "Encapsulation of bromocresol green pH indicator into a sol-gel matrix," *Journal of Dispersion Science and Technology*, vol. 26, no. 6, pp. 757–761, 2005.

[77] M. Bhanuprakash and S. Belagali, "Study of adsorption phenomena by using almond husk for removal of aqueous dyes," *Current World Environment*, vol. 12, no. 1, pp. 80–88, 2017.

[78] M. A. Palazzolo, P. D. Postemsky, and M. Kurina-Sanz, "From agro-waste to tool: biotechnological characterization and application of Ganoderma lucidum E47 laccase in dye decolorization. 3," *Biotech*, vol. 9, no. 6, p. 213, 2019.

[79] X. Feng, Y. He, H. Yang, and Y. Juan, "Self-adaptive bacterial foraging optimization algorithm based on evolution strategies," *Revista Tecnica de la Facultad de Ingenieria Universidad del Zulia*, vol. 39, no. 8, pp. 350–358, 2016.

[80] R. Lamaria, B. Benotmanea, and S. Mezalib, "Zeolite imidazolate framework-11 for efficient removal of bromocresol green in aqueous solution, isotherm kinetics, and thermodynamic studies," *Desalination and Water Treatment*, vol. 224, pp. 407–420, 2021.

[81] D. Phuong, N. Loc, and T. Miyanishi, "Efficiency of dye adsorption by biochars produced from residues of two rice varieties, Japanese Koshihikari and Vietnamese IR50404," *Desalination and Water Treatment*, vol. 165, pp. 333–351, 2019.

[82] Y. Liu, Y. Huang, A. Xiao, H. Qiu, and L. Liu, "Preparation of magnetic Fe_3O_4/MIL-88A nanocomposite and its adsorption properties for bromophenol blue dye in aqueous solution," *Nanomaterials*, vol. 9, no. 1, p. 51, 2019.